Surface & Coatings Technology 266 (2015) 64–69

Contents lists available at ScienceDirect

Surface & Coatings Technology

journal homepage: www.elsevier.com/locate/surfcoat

Tribocorrosion behaviors of AlN/MoS_2–phenolic resin duplex coatings on nitrogen implanted magnesium alloys

Zhiwen Xie [a,c], Tian Chen [a], Qiang Chen [b,*], Qin Yang [a], Sheng Tan [a], Yunjiao Wang [a], Yimin Luo [a], Zhuangzhu Luo [a], Minqi Hua [d]

[a] Chongqing Institute of Green and Intelligent Technology, Chinese Academy of Sciences, Chongqing 400714, China,
[b] Southwest Technology and Engineering Research Institute, Chongqing 400039, China
[c] University of Science and Technology Liaoning, Anshan 114051, China
[d] State Key Laboratory of Solid Lubrication, Lanzhou Institute of Chemical Physics, Chinese Academy of Sciences, Lanzhou 730000, China

ARTICLE INFO

Article history:
Received 11 June 2014
Accepted in revised form 7 February 2015
Available online 15 February 2015

Keywords:
Magnesium alloys
MoS_2–phenolic resin coating
Duplex structure
Tribocorrosion
Plasma immersion ion implantation and deposition

ABSTRACT

Nitrogen ion implantation and AlN/MoS_2–phenolic resin duplex coating are designed to improve wear and corrosion resistance of magnesium alloys. The microstructure and tribocorrosion behaviors of as-fabricated coatings are characterized by X-ray diffraction (XRD), scanning electron microscopy (SEM), Fourier transform infrared spectroscopy (FTIR), tribocorrosion and electrochemical tests. Studies show that Cl ions induce severe corrosion degradation of magnesium alloy during the tribocorrosion test. MoS_2–phenolic resin coating has two phase composite structure consisting of MoS_2 crystalline and phenolic resin, but this coating shows poor tribocorrosion resistance because force–corrosion synergy interaction accelerates the degradation process. The introduction of nitrogen ion implantation and AlN interlayer remarkably retards the corrosion degradation process of magnesium alloy. AlN/MoS_2–phenolic resin duplex coating exhibits better tribocorrosion resistance. These present results indicating that gradient duplex coating might be a good candidate as protective coating in engineering applications of magnesium alloys.

1. Introduction

In recent years, magnesium alloys have received extensive attention in automotive and aerospace industries due to their characteristic properties, including high strength-to-weight ratio, excellent damping capacity, high thermal conductivity, good manufacturability and potential recycling capability [1–3]. However, poor corrosion resistance and unsatisfactory wear performance of magnesium alloys restrict their industrial applications [4].

Surface modifications are an effective method to improve anti-wear and anti-corrosion properties of magnesium alloys. Ceramic coatings fabricated by microarc oxidation (MAO) can improve wear and corrosion resistance of magnesium alloys. However, these hard ceramic coatings usually exhibit a high friction coefficient and suffer from corrosion failure due to the growth defects such as micro-pores and cracks [5–7]. Ion implantation can improve corrosion resistance of magnesium alloys, but the implanted layers are not as effectively thick as ceramic coatings [8,9]. Hard coatings synthesized by physical vapor deposition (PVD) benefit wear resistance improvement of magnesium alloys [10–12], but galvanic corrosion always occurs between coatings and substrates due to a large potential difference [13]. In addition, these hard coatings also show unsatisfactory wear performance due to low load-bearing capacity of magnesium alloys [14]. Duplex coatings, such as (Ti:N)-DLC/MAO, have been shown to possess excellent wear and corrosion resistance [15–17]. These present results indicate that duplex architecture seems to be a possible choice to not only reduce the effect of galvanic corrosion but also hold high load-bearing capacity.

Phenolic resins have been widely used in automobile and aviation industries due to their superior mechanical strength and corrosion resistance [18,19]. However, poor wear resistance of phenolic resins limits their tribological applications [20]. Many studies have reported that adding various filling constituents into phenolic resins can significantly improve their wear resistance [21,22]. These present results indicating that phenolic resin-based self-lubricating coatings show a great promise prospect to improve wear and corrosion resistance of magnesium alloys. In this study, nitrogen ion implantation and AlN/MoS_2–phenolic resin duplex coatings are designed to improve wear and corrosion resistance of magnesium alloys. The purpose of nitrogen ion implantation is to induce densification of the oxide layer. AlN interlayer is used to retard galvanic corrosion and provide load support for soft MoS_2–phenolic

* Corresponding author at: No. 33 Yuzhou Road, Chongqing 400039, China. Tel.: +86 23 68792286; fax: +86 23 68792200.
E-mail address: 2009chenqiang@163.com (Q. Chen).

http://dx.doi.org/10.1016/j.surfcoat.2015.02.013
0257-8972/

Table 1
Experimental details of as-fabricated coatings.

Sample	Coatings
M0	AM60 substrate
M1	AM60 substrate/MoS_2–phenolic resin coating
M2	Nitrogen implanted AM60 substrate/AlN/MoS_2–phenolic resin coating

resin layer. In addition, the microstructure and tribocorrosion behaviors of as-fabricated coatings are investigated in detail.

2. Materials and methods

Si wafers and AM60 magnesium alloys are used as the substrate. The samples are mechanically polished by diamond paste and ultrasonically washed by using pure ethanol. High purity Al (99.99%) is as the targets. High purity nitrogen is as the working atmosphere. Nitrogen ion implantation and AlN interlayer are carried out in a plasma immersion ion implantation and deposition facility [23]. Prior to ion implantation, all the samples are cleaned by Ar+ sputtering at a bias voltage of 6 kV for 30 min to remove residual pollution and surface native oxide. Ion implantation is conducted in nitrogen atmosphere. Nitrogen plasma is produced by a radio-frequency method. Immersion ion implantation is conducted by applying a high pulsed bias voltage. The implantation parameters are displayed as follows, nitrogen flow — 50 sccm, pressure — 0.6 Pa, bias voltage — 30 kV, frequency — 200 Hz, bias voltage

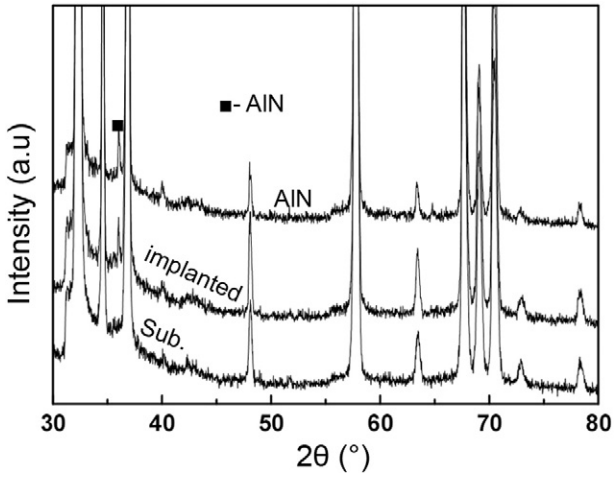

Fig. 1. XRD patterns of substrate, nitrogen implanted substrate and AlN interlayer.

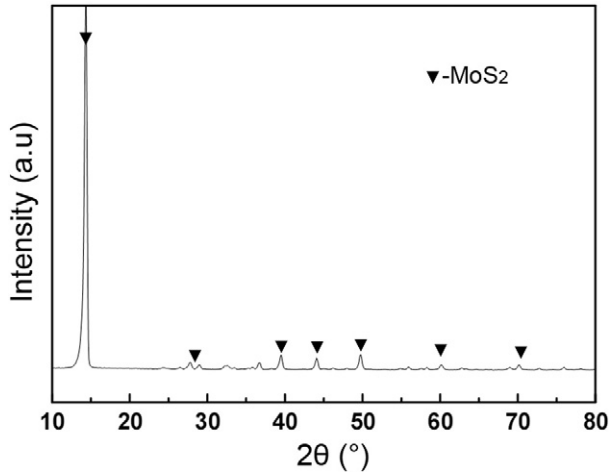

Fig. 2. XRD pattern of MoS_2–phenolic resin coating.

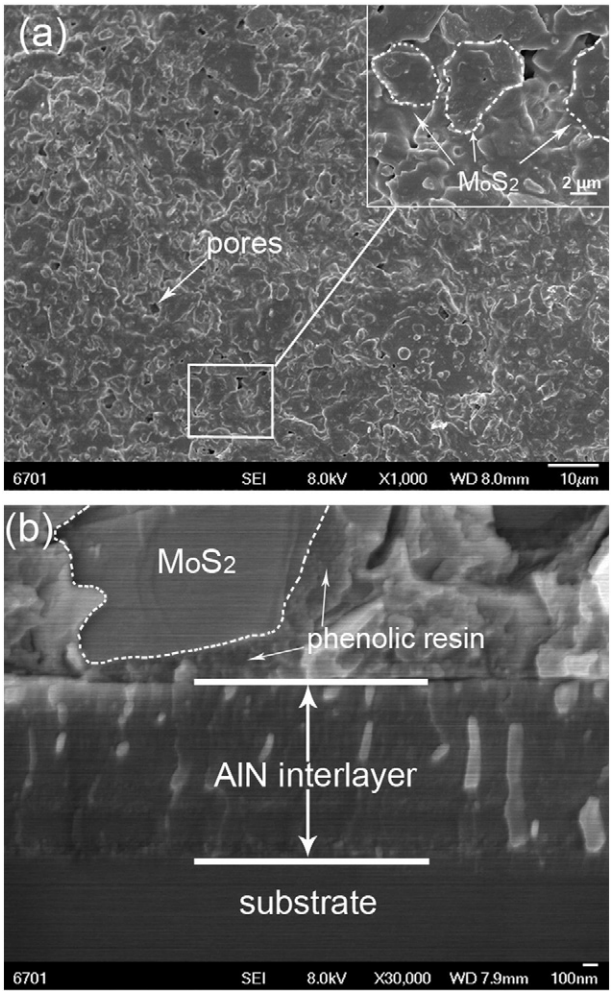

Fig. 3. (a) SEM surface image of MoS_2–phenolic resin coating; (b) SEM cross-section image of sample M2.

duration time — 20 μs and time — 2 h. Afterwards, the AlN interlayer is deposited on the surface of the implanted sample in nitrogen atmosphere. The Al metal plasma is produced by a pulse cathodic arc plasma source and is guided into the chamber through a magnetic filter duct. The metal plasma reacts with nitrogen plasma to form the AlN interlayer. The experimental parameters were displayed as follows, pressure — 0.3 Pa, bias voltage — 20 kV, frequency — 50 Hz, bias voltage

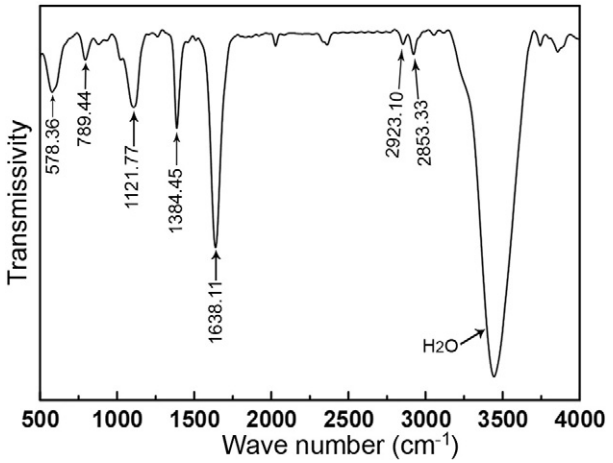

Fig. 4. FTIR spectrum of MoS_2–phenolic resin coating.

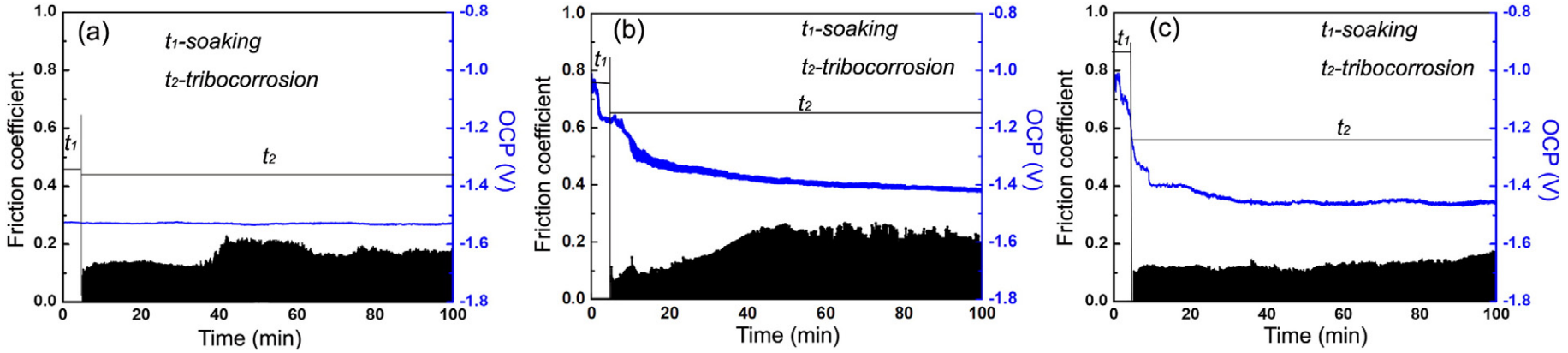

Fig. 5. Tribocorrosion curves with corresponding OCP of all samples: (a) M0; (b) M1; and (c) M2.

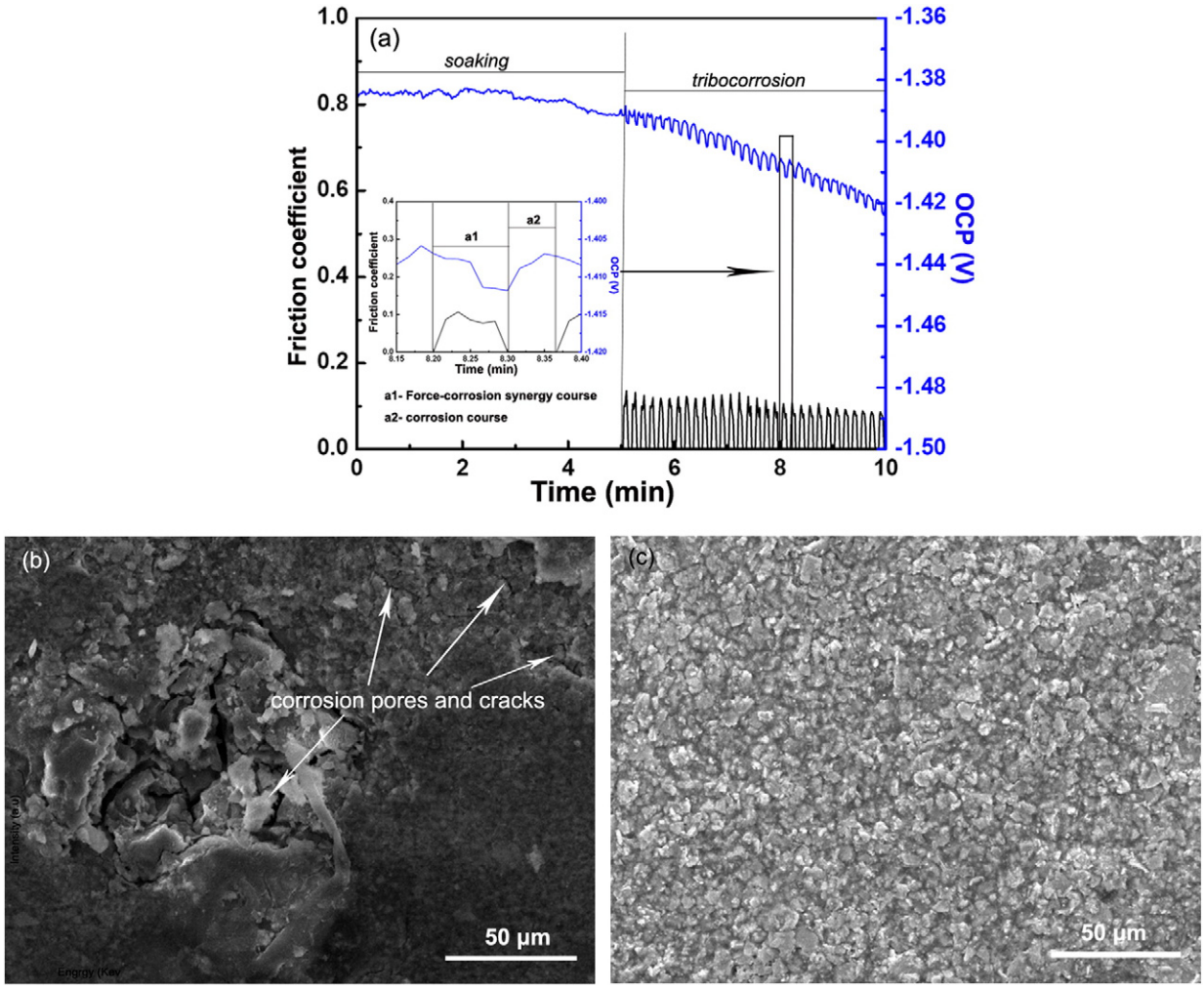

Fig. 6. (a) Tribocorrosion curves of sample M1; (b) wear scar morphology of sample M1; and (c) surface morphology of sample M1 after 30 min soaking test.

duration time — 60 μs, N_2 flow — 50 sccm and deposition time — 5 h. The top MoS_2–phenolic resin layer is fabricated by mechanical spraying. High purity micron-scale MoS_2 powders and phenolic resin are added to the organic solvent in a certain proportion. The mixed solutions are dispersed under sonication for 1 h. The coated samples are solidified in a sintering furnace. The curing temperature is 180 °C and curing time is 90 min. The experimental details of as-fabricated duplex coatings are given in Table 1.

The crystalline structure of as-fabricated coatings is determined by X-ray diffraction (XRD, Philips-X'pert) using Cu Kα radiation source. Scanning electron microscopy (SEM, JSM-6701F) is employed to observe the surface and cross section morphologies of as-fabricated coatings. Fourier transform infrared spectroscopy (FTIR, Nicolet) is used to investigate the bonding state in MoS_2–phenolic resin coating. The corrosion behaviors of as-fabricated coatings are evaluated by electrochemical test (PGSTAT302N). High purity platinum is as the counter electrode, the samples are as the working electrode (1 cm^2 exposed areas) and a saturated calomel electrode (SCE) is as the reference electrode. The test was carried out in a 1 M NaCl solution. The tribocorrosion behaviors of as-fabricated coatings are evaluated by a ball on-disk reciprocating sliding tribometer (MFT-R4000). High purity graphite is as the counter electrode, the sample is as the working electrode and a saturated calomel electrode (SCE) is as the reference electrode. All tribocorrosion tests are carried out in a 1 M NaCl solution. A 5 N load is applied on the sample through a Si_3N_4 ball (Φ6 mm). The amplitude and frequency are 5 mm and 0.1 Hz, respectively. Each test is repeated three times under the same conditions in order to check the reproducibility. The wear scar morphologies with corresponding compositions are examined by scanning electron microscope (SEM).

3. Results and discussion

Fig. 1 shows the XRD patterns of substrate, nitrogen implanted substrate and AlN interlayer. Deducting the signals of magnesium substrate from XRD patterns, AlN (002) peaks can be easily identified in nitrogen implanted substrate and AlN interlayer, which are in accordance with previous results that AlN tends to present the (002) preferred texture [24].

Fig. 2 shows the XRD pattern of MoS_2–phenolic resin coating. The main refection angles (2θ) locate at 14.32°, 29.02°, 32.68°, 35.89°, 39.49°, 44.15°, 49.79°, 60.17° and 70.14°, which are associated with MoS_2 (002), (004), (100), (102), (103), (006), (105), (008) and (108), respectively. The XRD result indicates that MoS_2 crystalline forms in as-fabricated MoS_2–phenolic resin coating.

SEM surface image presented in Fig. 3a shows that MoS_2–phenolic resin coating exhibits uniform surface dispersed with micrometer-sized MoS_2 particles. In addition, plenty of visible micro-pores are observed on the surface of MoS_2–phenolic resin coating, indicating poor coating density. As shown in Fig. 3b, AlN/MoS_2–phenolic resin duplex coating has a two layered structure. The thickness of the AlN interlayer is about 1.14 μm.

The FTIR spectrum of the MoS_2–phenolic resin coating is shown in Fig. 4. The band located at 1121.77 cm^{-1} corresponds to O–H groups. The band centered at 1384.45 cm^{-1} is for C–C groups. The peaks located

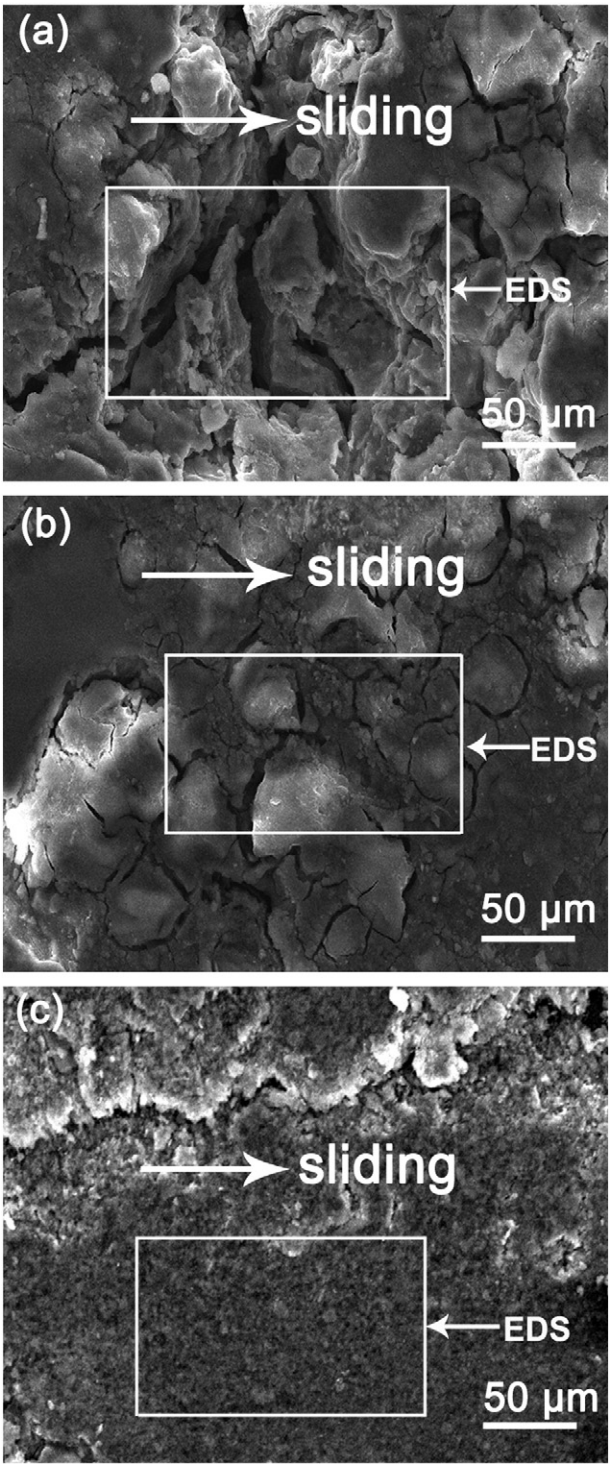

Fig. 7. SEM wear scar morphologies of all samples: (a) M0; (b) M1; and (c) M2.

at 2923.10 cm^{-1} and 2853.33 cm^{-1} are assigned to C–H_2 and C–H groups, respectively. The bands located at 1638.11 cm^{-1}, 720.44 cm^{-1}, 578.36 cm^{-1} and 462.07 cm^{-1} can be assigned to benzene rings, respectively. According to the XRD, SEM and FTIR results, we can conclude that MoS_2–phenolic resin coating has a two phase composite structure which is MoS_2 crystalline embedded in the phenolic resin matrix.

Fig. 5 shows the tribocorrosion curves with corresponding open circuit potentials (OCP) of all the samples. As shown in Fig. 5a, sample M0 possesses an unstable friction coefficient during the tribocorrosion period, but it remains relatively stable OCP of −1.53 V during the soaking and tribocorrosion period. The friction coefficient of sample M1 is 0.11 at initial stage and increases to 0.23 as the sliding time is more than 20 min. The corresponding OCP of sample M1 decreases by 0.14 V during the soaking period and 0.31 V during the tribocorrosion period (Fig. 5b). In comparison to that of sample M1, sample M2 exhibits a stable friction coefficient of 0.13 during the whole tribocorrosion period, indicating a better tribocorrosion resistance. The corresponding OCP of sample M2 decreases by 0.17 V during the soaking period and 0.29 V during the tribocorrosion period (Fig. 5c).

Table 2
Compositions at wear scars of as-fabricated coatings.

Sample	Mg (at.%)	Al (at.%)	S (at.%)	Mo (at.%)	Cl (at.%)
M0	67.86	10.35	–	–	21.79
M1	66.74	7.12	2.89	2.48	20.77
M2	2.87	9.11	47.63	35.03	5.36

The SEM observation shown in Fig. 3a shows that plenty of micropores distribute on the surface of the MoS_2–phenolic resin coating. These growth defects are likely as a diffusion channel for corrosive media and eventually lead to the OCP decline of samples M1 and M2. However, the reduction value during the tribocorrosion period is much higher than that during the soaking period (Fig. 5b and 5c). This phenomenon can be attributed to force–corrosion synergy interaction. As shown in Fig. 6a, the OCP of sample M1 exhibits an obvious declining trend during the tribocorrosion period. The magnified curve inserted in Fig. 6a shows that the OCP decreases during the tribocorrosion test (a1 stage) and increases significantly as the friction coefficient reduces to zero (a2 stage). The SEM image presented in Fig. 6b shows that some visible corrosion pores and cracks are observed on the wear scar, but these corrosion defects are absent from the surface of sample M1 after 30 min soaking (Fig. 6c). These above results confirm that force–corrosion synergy interaction accelerates the corrosion failure process of MoS_2–phenolic resin coating.

Fig. 7 shows the wear scar morphologies of all the samples after the tribocorrosion test. The corresponding compositions determined by EDS are presented in Table 2. As shown in Fig. 7a, plenty of corrosion defects are observed and high Cl content of 21.79% is identified in the wear scar of sample M0, indicating severe Cl ion corrosion degradation [1]. These visible corrosion defects are also observed on the wear scar of sample M1 (Fig. 7b), indicating that this coating has worn out. In addition, a large number of Mg (66.74%) and Cl (20.77%) are identified in the wear scar of sample M1, indicating that severe degradation occurs during the tribocorrosion test. In comparison to that of sample M1, the wear scar of sample M2 is very smooth and a large number of S (47.63%) and Mo (35.03%) are identified, hinting that this coating exhibits better tribocorrosion resistance (Fig. 7c).

The influence of nitrogen implantation/AlN interlayer on corrosion resistance of magnesium alloy is investigated by electrochemical test. Fig. 8 shows the polarization curves with corresponding corrosion morphologies. As shown in Fig. 8a, the magnesium alloy has a corrosion potential of −1.39 V and a corrosion current density of 8.89×10^{-5} A/cm^2. In comparison, nitrogen implantation/AlN interlayer exhibits a better corrosion resistance with a higher corrosion potential of −0.95 V and a lower corrosion current density of 4.32×10^{-7} A/cm^2 (Fig. 8b). The SEM image presented in Fig. 8 shows that plenty of corrosion defects are observed on the surface of magnesium alloy. However, nitrogen implantation/AlN interlayer exhibits smooth morphology except for some pitting corrosion pores. Electrochemical test confirms that nitrogen implantation and AlN interlayer effectively retard the corrosion degradation of magnesium alloy.

According to the tribocorrosion and electrochemical results, the magnesium alloy is sensitive to Cl ions and severe corrosion degradation occurs simultaneously during the tribocorrosion period. MoS_2–phenolic resin coating exhibits poor tribocorrosion resistance, which can be attributed to force–corrosion synergy interaction. As shown in Fig. 6, the

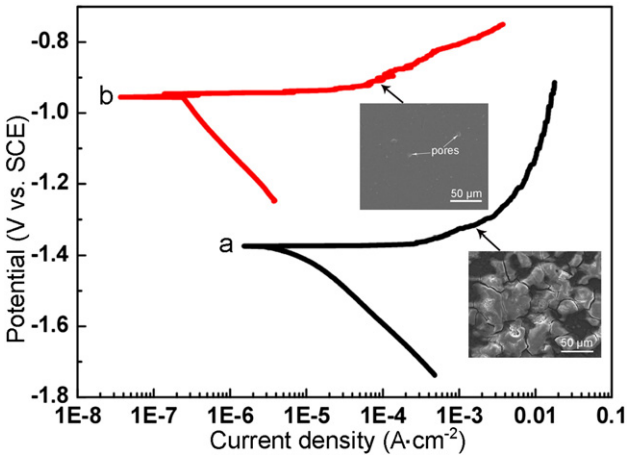

Fig. 8. Polarization curves with corresponding corrosion morphologies of (a) magnesium alloy and (b) nitrogen implantation/AlN interlayer.

force–corrosion synergy interaction accelerates the corrosion degradation process of the substrate. Severe degradation weakens the interfacial adhesion strength and eventually leads to the tribocorrosion failure of the MoS_2–phenolic resin coating. In comparison, the AlN/MoS_2–phenolic resin duplex coating exhibits a better tribocorrosion resistance, which can be attributed to nitrogen ion implantation and AlN interlayer. Nitrogen ion implantation induces densification of the oxide layer and the formation of AlN phase [25]. The AlN interlayer inhibits galvanic corrosion because its potential is closer to that of the substrate [24]. As a result, nitrogen implantation/AlN interlayer effectively retards the corrosion degradation process of magnesium alloy (Fig. 8). The top MoS_2–phenolic resin remains a high adhesion strength with AlN interlayer and excellent tribocorrosion resistance is achieved in the as-fabricated AlN/MoS_2–phenolic resin duplex coating.

4. Conclusions

This study investigates the microstructure and tribocorrosion behaviors of AlN/MoS_2–phenolic resin duplex coatings fabricated on the nitrogen implanted magnesium alloy, and the main conclusions are listed as follows:

(1) The Magnesium alloy is sensitive to Cl ion and a serious corrosion degradation occurs simultaneously during the tribocorrosion test.
(2) MoS_2–phenolic resin coating has a two phase composite structure which is MoS_2 crystalline embedded in the phenolic resin matrix.
(3) Single MoS_2–phenolic resin coating exhibits a poor tribocorrosion resistance because the force–corrosion synergy interaction accelerates the corrosion failure process.
(4) The nitrogen ion implantation and AlN interlayer remarkably retard the corrosion process of magnesium alloy. The AlN/MoS_2–phenolic resin duplex coating exhibits a better tribocorrosion resistance.

Acknowledgment

This work is supported by the National Natural Science Foundation of China (No. 51401201), the Chinese Academy of Sciences Western Light (No. Y32Z010F10) and the Enterprise Cooperation Project (No. Y32H130F10). We gratefully acknowledge Prof. L. P. Wang, Harbin Institute of Technology, for helpful discussions and contributions during the coating preparation.

References

[1] H. Hoche, H. Scheerer, D. Probst, E. Broszeit, C. Berger, Surf. Coat. Technol. 174–175 (2003) 1018–1023.
[2] Q. Chen, Z.X. Zhao, D.Y. Shu, Z.D. Zhao, Mater. Sci. Eng. A 528 (2011) 3930–3934.
[3] Q. Chen, S.J. Luo, Z.D. Zhao, J. Alloys Compd. 477 (2009) 726–731.
[4] J.E. Gray, B. Luan, J. Alloys Compd. 336 (2002) 88–113.
[5] E.E. Demirci, E. Arslan, K.V. Ezirmik, Ö. Baran, Y. Totik, İ. Efeoglu, Thin Solid Films 528 (2013) 116–122.
[6] H.F. Guo, M.Z. An, S. Xu, H.B. Huo, Mater. Lett. 60 (2006) 1538–1541.
[7] J. Liang, P.B. Srinivasan, C. Blawert, W. Dietzel, Corros. Sci. 51 (2009) 2483–2492.
[8] H.X. Liu, Q. Xu, D.M. Xiong, B. Lin, C.L. Meng, Vacuum 89 (2013) 233–237.
[9] Y. Zhao, G.S. Wu, Q.Y. Lu, J. Wu, R.Z. Xu, K.W.K. Yeung, P.K. Chu, Thin Solid Films 529 (2013) 407–411.
[10] Y.J. Shi, S.Y. Long, S.C. Yang, F.S. Pan, Vacuum 84 (2010) 962–968.
[11] W. Dai, G.S. Wu, A.Y. Wang, Diamond Relat. Mater. 19 (2010) 1307–1315.
[12] F. Hollstein, R. Wiedemann, J. Scholz, Surf. Coat. Tech. 162 (2003) 261–268.
[13] H. Hoche, C. Blawert, E. Broszeit, C. Berger, Surf. Coat. Tech. 193 (2005) 223–229.
[14] N. Yamauchi, K. Demizu, N. Ueda, N.K. Cuong, T. Sone, Y. Hirose, Surf. Coat. Tech. 193 (2005) 277–282.
[15] Z.W. Xie, Z.Z. Luo, Q. Yang, T. Chen, S. Tan, Y.J. Wang, Y.M. Luo, Vacuum 101 (2014) 171–176.
[16] W. Yang, P.L. Ke, Y. Fang, H. Zheng, A.Y. Wang, Appl. Surf. Sci. 270 (2013) 519–525.
[17] J.F. Zhang, W. Zhang, C. Yan, K. Du, F.H. Wang, Electrochim. Acta 55 (2009) 560–571.
[18] C.T. Lin, H.T. Lee, J.k. Chen, Appl. Surf. Sci. 284 (2013) 297–307.
[19] C.P. ReghunadhanNair, Prog. Polym. Sci. 29 (2004) 401–498.
[20] G.W. Yi, F.Y. Yan, Wear 262 (2007) 121–129.
[21] M.H. Cho, J.J.S.J. Kim, H. Jang, Wear 260 (2006) 855–860.
[22] S. Betancourt, L.J. Cruz, A. Toro, Wear 272 (2011) 43–49.
[23] L.P. Wang, L. Huang, Z.W. Xie, X.F. Wang, B.Y. Tang, Rev. Sci. Instrum. 79 (2008) 023306.
[24] G.S. Wu, W. Dai, H. Zheng, A.Y. Wang, Surf. Coat. Tech. 205 (2010) 2067–2073.
[25] G.S. Wu, K.J. Ding, X.Q. Zeng, X.M. Wang, S.S. Yao, Scripta Mater. 61 (2009) 269–272.